

A Comparison of the Heat Transfer Performance of a Hexagonal Pin Fin with Other Types of Pin Fin Heat Sinks

Eaman Hassan Muhammad

Assistant Lecturer, University of Wassit/College of Engineering

Abstract: In this study, the heat transfer performance of hexagonal pin-fin heat sinks is compared with various commonly used fin geometries in laminar forced convection. Overall the numbers of models are carried out during this study 8 different model. In other words, 4 models in in-line arrays and the other in staggered arrays, which were round, square, rectangular and the case study hexagonal. In order to compare these various geometries, a set of standard conditions was required, the basic conditions used here (3.3mm) hydraulic diameter and (6.6mm) pitch were the same in all shapes. The ratio (PL/PW) was chosen to be one. The Analysis was simplified by some major assumptions. The fluid in the domain is air. The compressibility effects are ignored due to the low air speed. Heat transfer and fluid flow were assumed to be two-dimensional, with identical velocity and pressure distribution in the z-direction. The ratio of solid to fluid thermal conductivity for aluminum and air is around 8360, permitting the fins to be modeled as isothermal surfaces rather than conjugate solids. Numerical simulations are performed using FLUENT 6.3. The CFD simulations were carried out on a two-dimensional computational domain bounded by planes of symmetry parallel to the flow. The air approach velocity was in the range of 0.165 to 4.5m/s. A comparison of heat transfer performance and pressure drop is presented. In general, for the given pressure gradient and flow rate, the hexagonal fin geometry yield a higher Nusselt number in comparison to square fins, and a lower Nusselt number in comparison to circular fins. And it can be noted that the staggered hexagonal fin geometry gave the heat transfer performance like in-line circular performance at most Reynolds numbers in the range considered here.

Keywords: Electronic Cooling , Computational Fluid Dynamics, laminar flow , Pin fin Heat Sink Electronic Cooling, pin Fin, Heat sink, CFD laminar flow

Nomenclature

C_f Friction coefficient
 C_p Specific heat capacity (J/g °C)
 D_h Hydraulic diameter (mm)
 h Surface heat transfer coefficient (W/m² K)
 k Thermal conductivity of air (W/m K)
 Nu Nusselt number
 P Wetted perimeter of the cross-section
 P_L Lengthwise pitch (mm)
 P_w Spanwise pitch (mm)
 $(\Delta P/L)$ Pressure drop per unit length (Pa/m)
 Re Reynolds number
 u, v Components of the velocity vector
 v_{app} Heatsink approach velocity (m/s)
 x, y Cartesian coordinates
Greek symbol
 ρ Density of air (kg/m³)
 μ Dynamic viscosity of air (kg/m s)

1. Introduction

The fast development of high-density microelectronic circuits requires more effective ways of cooling the microchips and other microelectronic devices, electronic packagers have underlined the need for employing effective cooling devices and cooling methods to maintain the operating temperatures of electronics components at a safe and satisfactory level.

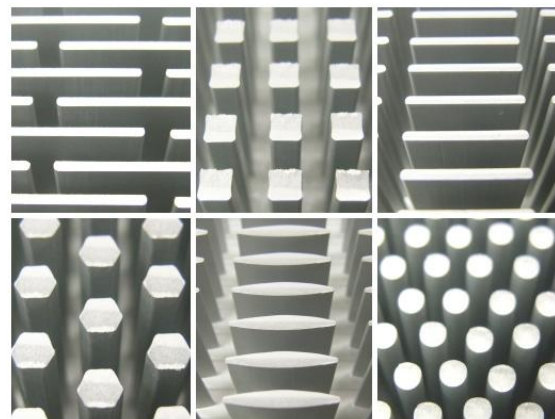


Figure 1: Types of pin fin heat sink

The heatsink industry, traditionally the supplier of cooling products, is always searching for new technologies which enhance thermal performance with no cost penalties. For this reason, a comparison of various geometries of pin fin heatsinks is of interest and needs to be carried out to determine applicability as a general cooling product. Realistic, manufacturable geometries are considered for minimizing thermal resistance at moderate laminar air velocities and pressure gradients. These consist of plate fins or pin fins, which can be round, elliptical, or square. The plate fins can be continuous (parallel plates) or staggered. The pin fins can be in-line or staggered arrays as appears in Fig (1).

Sparrow and Larson[1] performed experiments to determine per fin heat transfer coefficients for a pin fin array situated in an oncoming longitudinal flow that turns to a cross-flow. They varied the geometric parameters of round fins

including the fin height to diameter ratio (H/D) and the inter-fin pitch to diameter ratio (P/D). The pressure drop across the array was also measured and presented in dimensionless form relative to a specially defined velocity head, which gave a universal pressure drop result for all operating conditions. Subsequent to this study, they also compared the performance of different pin fin geometries [2]. However, the objective was to determine which fin height and inter fin spacing yield the lowest overall thermal resistance for the array. The minimization of the resistance was sought under the constraint of constant pumping power for all candidate systems (i.e. those characterized by different H/D and P/D values) and for a uniform fin-to-airstream temperature difference for all fins in a given array, while forced convection through parallel plate fins studied by Keyes [3].

The optimal geometry of an array of fins that minimizes the thermal resistance between the substrate and the flow forced through the fins was reported by Bejan and Morega[4]. Both round pin fin arrays and staggered plate fin arrays were optimized in two steps, first the optimal fin thickness was selected and then the optimal size of fluid channel was determined. They also compared the minimum thermal resistance of staggered plate arrays and parallel plate fins. Furthermore, the dimensionless pressure gradient was plotted against Reynolds number.

In the experiments of Chapman et al.[5] with elliptical pin-fin heatsinks, results were obtained with aluminum heatsink made of extruded fin, crosscut rectangular fins, and elliptical fins in laminar air flow. All three heatsinks have equal volume, and the total surface area was also calculated to be nearly identical. The heatsink and ambient temperature difference was used to calculate thermal resistance. They supposed that the elliptical pin fin heatsink was designed to minimize the pressure loss across the heatsink by reducing the vortex effects and to enhance the thermal performance by maintaining large exposed surface area available for heat transfer.

Wirtz et al.[6] also studied the effect of flow bypass on the performance of longitudinal fin heatsinks, but Iwasaki et al.[7] studied the cooling performance of this typical heatsink by using numerical, experimental and nodal network techniques., while natural convection in the same geometry was studied by Culham et al.[8].

Wirtz and Colban[9] simulated electronic packages to compare the cooling performance of in-line and staggered plate arrays for both sparse and dense packaging configurations. They found that staggered arrays exhibit higher element heat transfer coefficients and friction factors than in-line arrays at a given flow rate. However, no significant difference in performance was observed between staggered and in-line configurations when they were compared based on either equal coolant flow pressure drop or pumping power. They did not change the element or channel geometry and therefore the effect of these parameters on their results is not known.

In-line and staggered plate arrays were also investigated, both numerically and experimentally, by Sathyamurthy et al.[10]. They obtained a good agreement between their

numerical results and experiments. Their results illustrated that the thermal performance of the staggered fin configuration was better than the planar fin configuration over the power and flow ranges examined. This enhanced thermal performance, however, was realized at the expense of an additional pressure drop.

Wirtz et al.[11] were amongst the earliest ones to measure the performance of a pin fin heatsink. In their work, experimental results were reported on the thermal performance of model fan-sink assemblies consisting of a small axial flow fan for impingement of air on a square array of pin fins. Cylinder, square, and diamond shape cross-section pin-fins were considered. The overall heatsink thermal resistances, R , were evaluated at fixed applied pressure rise and fixed fan power. They concluded that cylindrical pin fins give the best overall fan-sink performance. Elliptical pin fin arrays were not studied in their investigation. In addition, only impinging flow drawn through the fin arrays was considered.

Heat transfer enhancement mechanisms in in-line and staggered parallel plate fin heat exchangers were also studied by Zhang et al.[12] who examined the geometrical effects. There are also a few reports on the thermal performance and the flow bypass effects of parallel plate fin arrays. Barrett and Obinelo[13] studied tip clearance and spanwise spacing across a range of approach flow rates and fin densities. Lastly Soodphakdee et al [14] compared the round, elliptical, and plate fins in staggered and in-line configurations without considering that the fins hexagon.

Through previous studies, we can see that it did not address the form of hexagon, then we need to study the hexagonal pin fin and compared it with the rest of the commonest forms such as circular, square and rectangle pin fin where we proposed last (rectangle) and comparison to the purpose of determining the best performance. For a comparison of heatsink geometries, equal wetted perimeter of the fins per base area will be used. The present work is meant to be a generalized comparison in which the effects of flow parameters (e.g. pressure drop) on the heatsink performance are investigated in terms of thermal resistance between the heatsink surfaces to the ambient air. The mechanisms that influence the heat transfer and pressure drop of various pin fin heatsinks need to be understood.

The available literature on various thermal performance studies is briefly reviewed in both parallel flow and impinging flow configurations. The numerical simulation procedure used in this work is described and results of various configurations are compared.

2. CFD Models and Simulation

Computational fluid dynamics (CFD) is one of the branches of fluid mechanics that uses numerical methods and algorithms to solve and analyze problems that involve fluid flows. The numerical solver codes are well-established and thus provide a good start to more complex heat transfer and fluid flow problems. FLUENT provides adaptability to variation of thermo physical properties with respect to temperature effect. The fundamental basis of any CFD

problem is the Navier-Stokes equations, which define any single-phase fluid flow. These equations can be simplified by removing terms describing viscosity to yield the Euler equations. Further simplification, by removing terms describing vorticity yields the full potential equations. Finally, these equations can be linearized to yield the linearized potential equations.

-The mass conservation equation in 2-D field (continuity)

$$\frac{\partial u}{\partial x} + \frac{\partial v}{\partial y} = 0 \quad (1)$$

Where u and v are the velocity components

-The 2-D momentum conservation equations in x and y direction respectively are;

$$\rho \left(u \frac{\partial u}{\partial x} + v \frac{\partial u}{\partial y} \right) = -\frac{\partial P}{\partial x} + \mu \left(\frac{\partial^2 u}{\partial x^2} + \frac{\partial^2 u}{\partial y^2} \right) \quad (2)$$

$$\rho \left(u \frac{\partial v}{\partial x} + v \frac{\partial v}{\partial y} \right) = -\frac{\partial P}{\partial y} + \mu \left(\frac{\partial^2 v}{\partial x^2} + \frac{\partial^2 v}{\partial y^2} \right) \quad (3)$$

-The 2-D energy conservation equation is :

$$\rho \cdot Cp \left(u \frac{\partial T}{\partial x} + v \frac{\partial T}{\partial y} \right) = k \left(\frac{\partial^2 T}{\partial x^2} + \frac{\partial^2 T}{\partial y^2} \right) \quad (4)$$

The first step of the solution process requires a geometry modeler and grid generator. In this study the software Gambit of Fluent Company was used. The Gambit software allows one to build and mesh any model simple and intuitive, yet it is versatile enough to accommodate a wide range of modeling applications. The rest of the steps will be always executed in Fluent.

The hydraulic diameter of a regular hexagon external flow is determined from the flow passage area as follows [15]:

$$D_h = \frac{4A}{P} = \frac{4 * 2.59807a^2}{6a} = 1.732053a \quad (\text{with } a = \text{edge length})$$

Where P is the wetted perimeter of the cross-section

$$Re = \frac{\rho v_{app} D_h}{\mu} \quad (5)$$

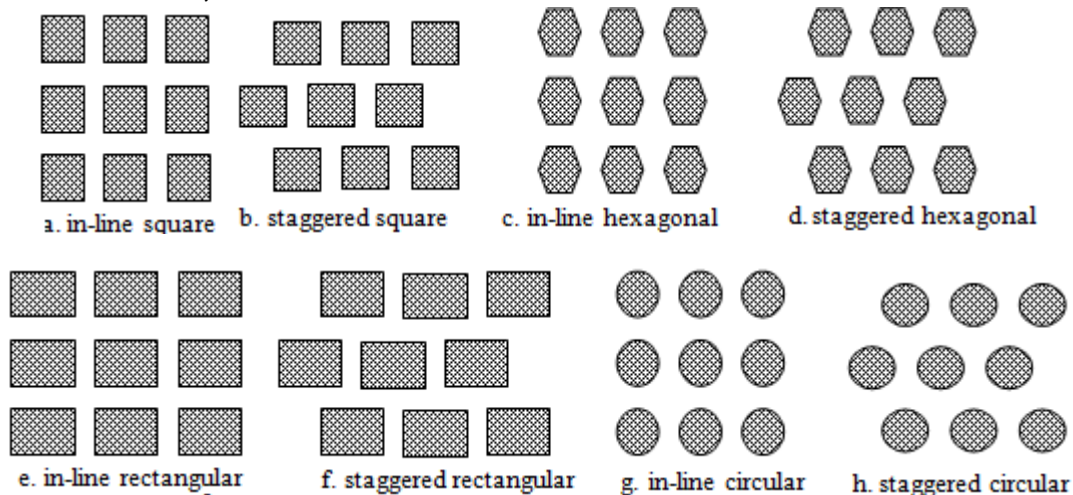


Figure 2: Schematic diagram of heatsinks

The Reynolds number (Re) is based on the hydraulic diameter and the heatsink approach velocity (v_{app}), (μ) Dynamic viscosity of air, (ρ) Density of air.

$$Nu = \frac{hD_h}{k} \quad (6)$$

For the Nusselt number, the bulk inlet temperature is used as the reference for heat transfer coefficient calculations, (h) Surface heat transfer coefficient, (k) Thermal conductivity of air.

Friction coefficient, C_f , is calculated as a function of pressure gradient in heatsink using heatsink approach velocity as reference [16]. The surface friction coefficient over an array of fins is defined as in equation (7).

$$C_f = \frac{(\Delta P / L) D_h}{4 \left(\frac{1}{2} \rho v_{app}^2 \right)} = \frac{(\Delta P / L) D_h}{2 \rho v_{app}^2} \quad (7)$$

where ($\Delta P/L$) is the pressure gradient (pressure drop in the fin array per unit length).

3. The Current Study

Most of the previous studies on pin fins or parallel plate fin heatsinks have considered an individual geometry. Although Chapman et al.[4] compared elliptical pin fin heatsink with crosscut pin fins and parallel plates, they used an equal volume of fins as the fixed parameter and Soodphakdee et al[14] compared different geometry of fins. Further, they did not include hexagonal and rectangular pin fins in their study. In this study, some of the issues didn't consider in the previous works will be addressed.

The objective is to numerically investigate the thermal performance of circular, square, hexagonal pin fin, and rectangular pin fin heatsinks and compare the results on a meaningful and fair basis. Both in-line and staggered arrays of different type fins are considered. Overall numbers of models are carried out during this study were 8 different models see Fig (2). In other words, 4 models in in-line arrays and the other four were used in staggered arrays as shown in table (1).

Table 1: Geometry of the heat sinks used in this research

Heat Sinks (mm)	D_h	P_L/P_W (mm)	Dimensions (mm ²)	Surface area (st. and inl. arrays)
Circular	3.3	1	$r=1.65$	10.362
Hexagonal	3.3	1	$a=1.906$	11.4
Square	3.3	1	$a=3.3, b=3.3$	13.2
Rectangle	3.3	1	$a=3.0, b=3.667$	13.334

This study investigates the performance of heat sinks numerically by simulating the case studies using GAMIT for the mesh generation, whereby the corresponding numerical solve is performed using Computational Fluid Dynamic software, FLUENT6.3.

A sample of the computational domain and grid for the hexagonal fin geometry is shown in Fig (3). The horizontal boundaries of the computational domain are symmetry boundary conditions. The computational module is assumed to be well within the bank of fins and hence the inlet and outlet boundaries are considered to be of a periodic type. To make it even more clearly, only the grid in the near of the fin is shown in Fig (3). The examine of mesh yield the total elements (15836) Active elements ratio (100%). The type of mesh used here is the triangle, pave with space (0.1). since the type of mesh fixed on all geometers.

The Computational Fluid Dynamics (CFD) code [17] is used. The code uses the Finite Volume method approach and employs the SIMPLE velocity-pressure coupling algorithm. The approach velocity range considered only covers laminar flow conditions.

Figure 3: Computational domain in-line and staggered and the grid near the hexagonal fin surface

4. Results and Discussions

To cover a fixed range of Reynolds numbers for each model, the results for the simulation of heat sink were obtained at various air velocities in the range of 0.165 to 4.5 m/s with a fixed hydraulic diameter. To validate the solution procedure, results of CFD simulations were compared with experimental data, detailed local measurements for most of the heatsink fin geometries simulated in this work are not available in the literature. Therefore, available experimental data were chosen such as experimental data done by Bergelin [18] for staggered tube, and Nishimura [19] for in-line tube banks.

A comparison of the local dimensionless surface shear stress for the flow around a staggered circular pin fin with experimental data is presented in Fig (4). It is noted that, the present work is in good agreement with experimental data, the mean deviation between simulation and experimental data was 22.3%. Fig (5) presents the variation of the dimensionless Heat Transfer Factor with Reynolds number in an in-line tube bank geometry, the latter comparison shows an unsatisfactory agreement (33%) between simulation and experimental data because the accuracy of the measurements between the experimental module and the numerical one, where the pitch ratio was 1.5 for the experimental case while it was 1 for the numerical one.

Fig (6) shows the variation of average Nusselt number with Reynolds number for the in-line and staggered geometries, the points on each curve correspond to six simulations carried out by varying the airflow rate. It's noted that the hexagonal fin shape shows better performance (high Nusselt number) than the square fin shape after circular fin shape, but it is interesting to note that the staggered hexagon is better than the in-line circular in range over Reynolds number 565. the lowest Nusselt number was for the in-line rectangle geometry, This result is not much different from the most previous research as shown in Fig (7) Ref.[14] where the staggered circular fin shape yields the highest Nusselt number at all Reynolds numbers in the range considered there.

Fig (8) shows comparison different geometries in pressure gradient versus Reynolds number. The different geometries can then be compared in terms of pressure gradient as a function of Reynolds number. At given Reynolds numbers, pressure drop increase with Reynolds number increasing and in-line circular lower in pressure drop than all cases and staggered circular lower than all cases in staggered arrangement. And the hexagonal shape fin was in the pressure drop less than square shape fin, but higher than circular shape fin. For clarity, the friction coefficient was plotted in Fig (9) for all cases without the rectangle one, where it seems clear the hexagon performance here, which mediates the performances of the square and circular in both arrangements, and the in-line circular and hexagonal were the lowest geometries.

In all cases the staggered arrangement has higher total heat transfer than in-line arrangement for the same Reynolds number as shown in Table(2). The in-line and staggered arrangements are seeing increasing in heat transfer and friction factor over a corresponding continuous fin geometries (which maintains the same heat transfer surface area) see table (1). For the case of in-line arrangement, the lateral gap between adjacent fins, which is available for flow see Fig (2). Thereby the velocity and temperature gradients are increased resulting in significant increase in the Friction Factor. But the velocity and temperature profiles approaching any fin element are not too far disturbed from the fully developed profile that the real boundary layer restart mechanism is not very strong in this case. For the case of staggered arrangement, the lateral gap between adjacent fin elements decreases only slightly due to the finite thickness of the fin. On the other hand, owing to the staggered arrangement the velocity and temperature profiles approaching any fin element are significantly distorted away from the fully developed profile. The resulting increased velocity and thermal gradients at the fin surface contribute to increase friction factor, where the Reynolds number is based on the hydraulic diameter and vortex shedding mechanisms, as well as the geometry effect arise from the finite thickness and the placement of the fin elements. These three effects together accounted for the substantial increasing in the friction factor. At a view to show the thermal performance, velocity profile and Vorticity see fig (10), and fig (11), (12).

5. Conclusions

The analysis of in-line and staggered pin-fin heat sinks is performed. The pressure drop and Nusselt number increases whereas Reynolds number increases, with approach velocity. The current study aims to compare the heat transfer performance of a hexagonal pin fin with various pin-fin heat sinks in eight models over a wide range of Reynolds numbers.

We find that the staggered circular fin shape yields the highest Nusselt number at all Reynolds numbers in the range considered here, and the lowest Nusselt number is for the in-

line rectangle pin fin, and the hexagonal fin shape shows better performance (high Nusselt number) than square fin shape, but it is interesting to note that the staggered hexagon is better than the in-line circular in range over Reynolds number 565, but the rectangle pin fin shape Less of square.

The hexagon performance in friction coefficient was mediates the performances of the square and circular in both arrangements, and the in-line circular and hexagonal were the lowest geometries. And total heat transfer rate was in the staggered arrangement higher than in in-line arrangement.

Table 2: Total heat transfer versus types of pin fins and Reynolds number

geometries	Total Heat Transfer Rate					
	Re=37	Re=113	Re=339	Re=565	Re=790	Re=1016.5
St. Circular	141.08	149.23	233.07	345.28	370.82	414.71
St.Hexagonal	151.36	159.38	251.72	352.27	376.96	434.01
St. Square	170.1	167.32	255.03	337.13	393.17	442.05
St.Rectangle	166.92	156.04	231.74	302.2	368.08	415.79
Inl.Circular	133.34	135.08	177.35	297.57	325.51	328.21
In.Hexagonal	143.3	144.43	181.37	285.38	302.1	320.07
Inl. Square	160.52	154.91	192.81	279.58	311.08	321.76
Inl.Rectangle	160.3	146.05	210.31	265.81	295.09	279.04

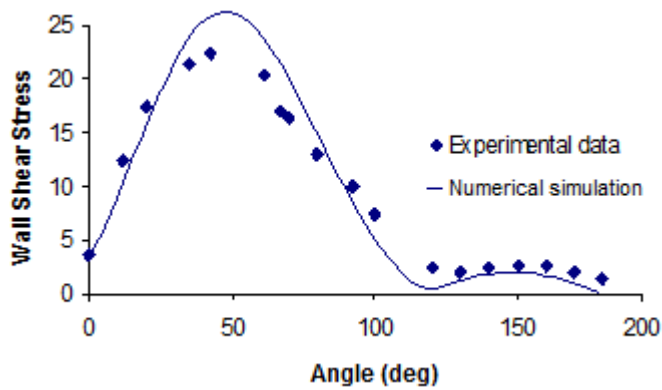


Figure 4: Comparison of experimental and numerical surface shear stress distributions at Re=54 for staggered Array of tubes

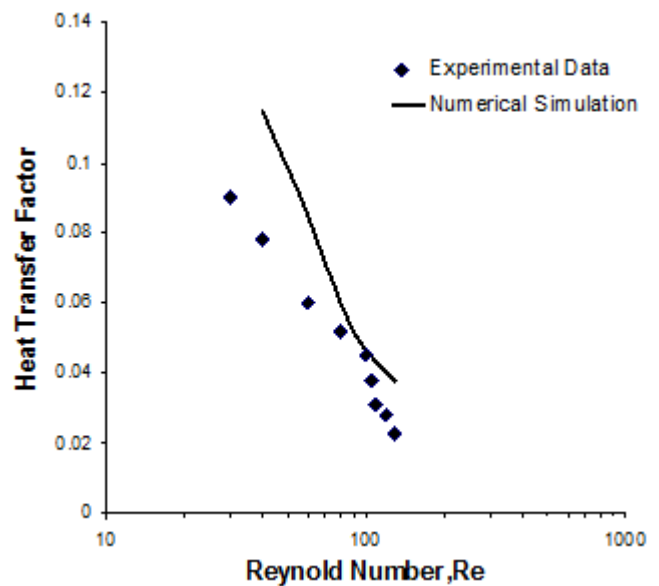


Figure 5: Comparison of experimental and numerical Heat Transfer Factor for an in-line array of tubes

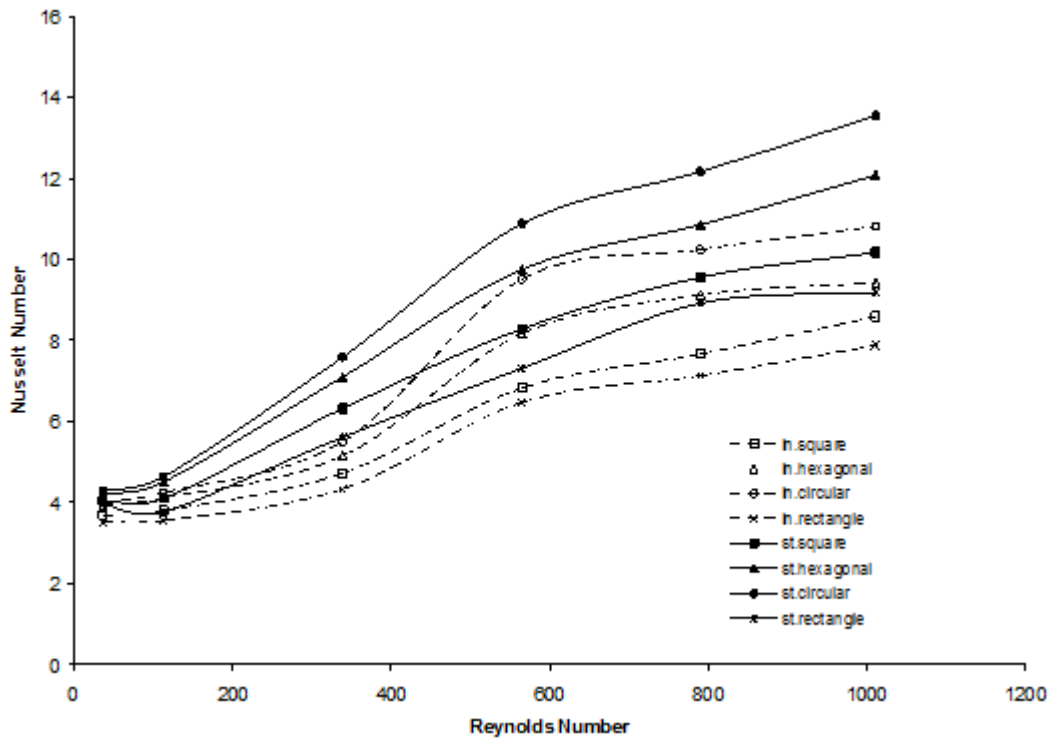


Figure 6: Average Nusselt number versus Reynolds number for various fin geometry.

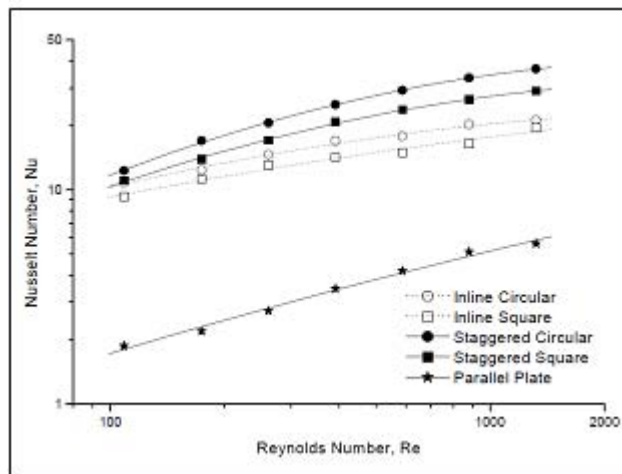


Figure7: Nusselt number versus Reynolds number for various fin geometries .by Soodphakdee [14]

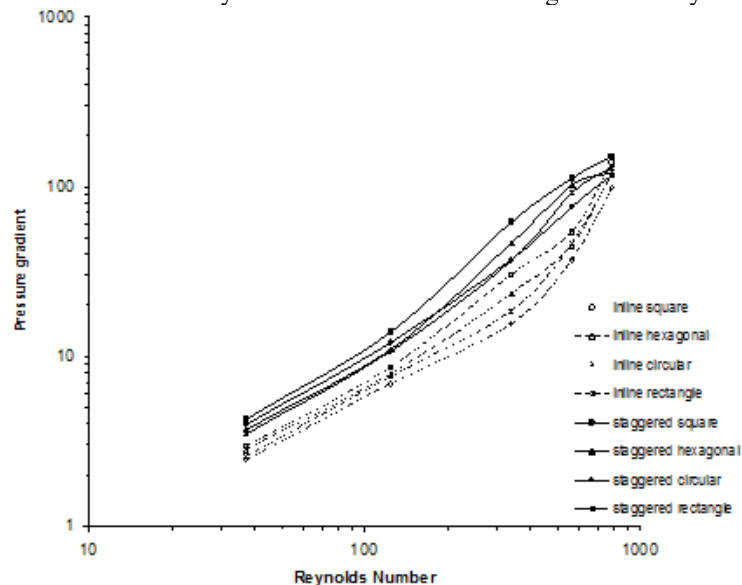


Figure 8: Pressure Gradient versus Reynolds number for various fin geometry

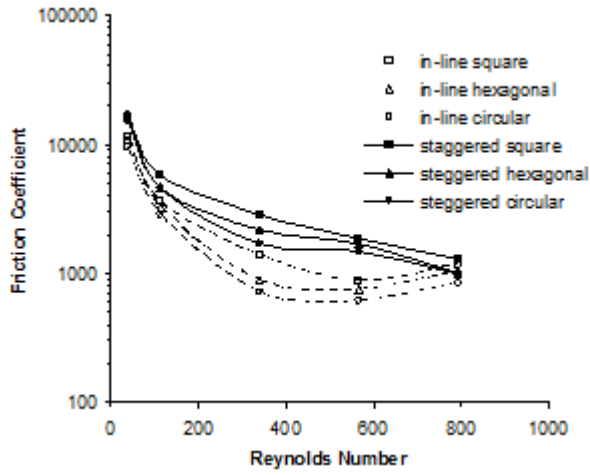


Figure 9: Friction coefficient versus Reynolds number for various fins.

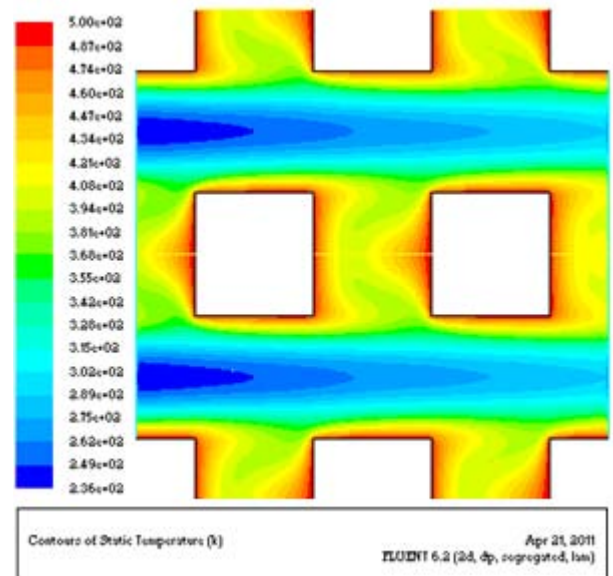


Figure 10 (c)

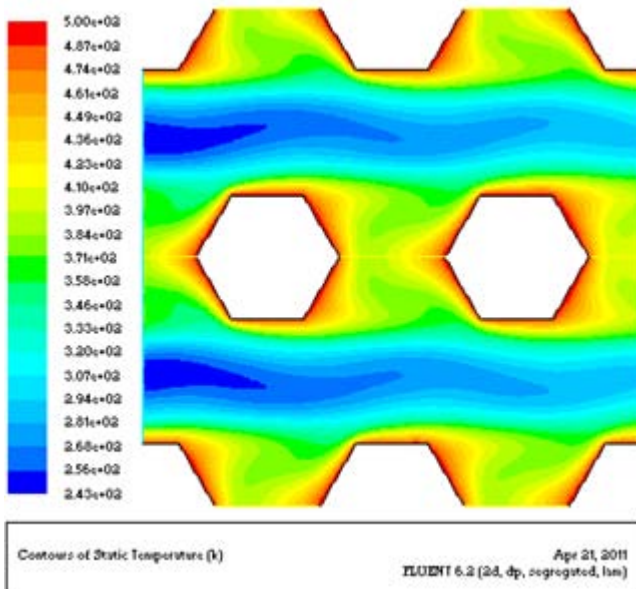


Figure 10 (a)

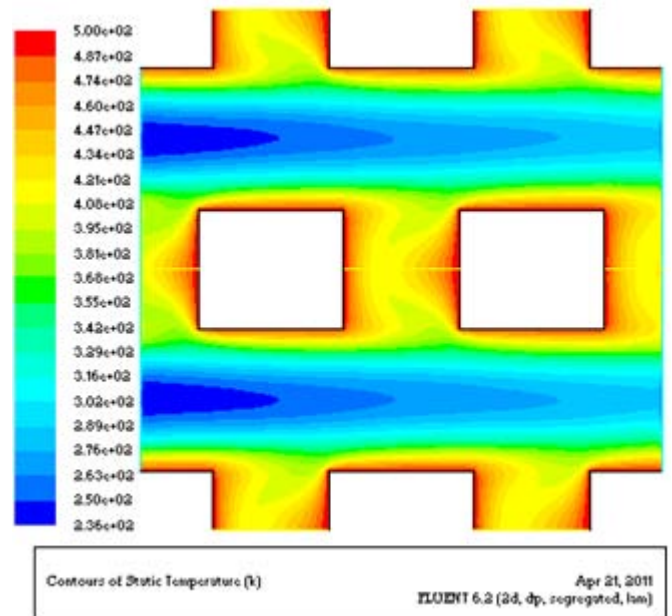


Figure 10 (d)

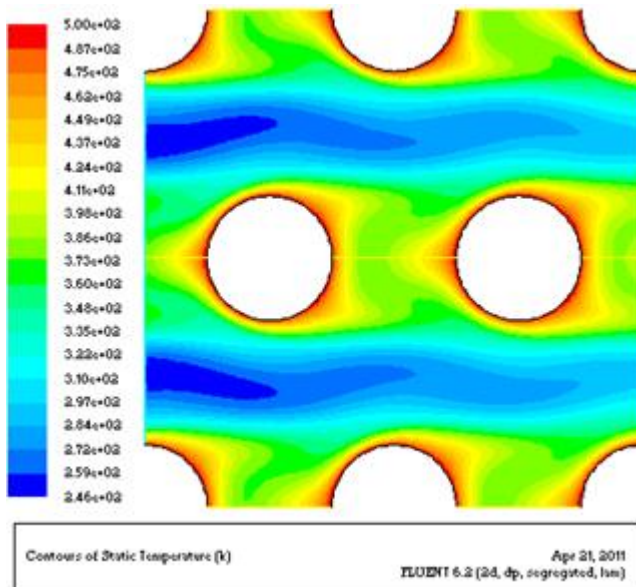
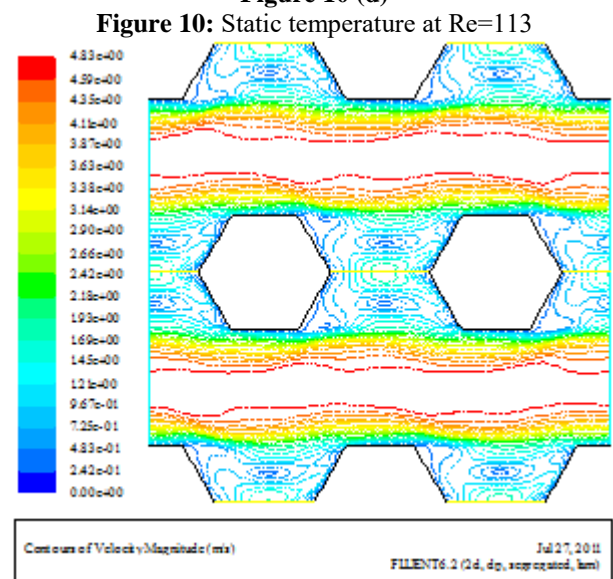
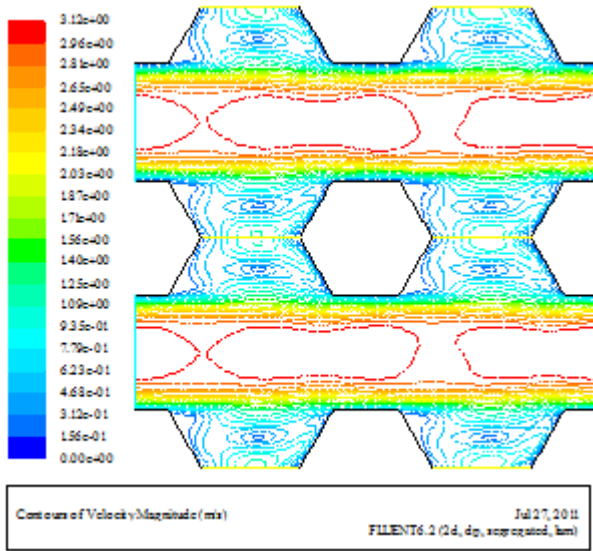


Figure 10 (b)



(a) Staggered



(b) in-line

Figure 11: Velocity Magnitude at Re=565

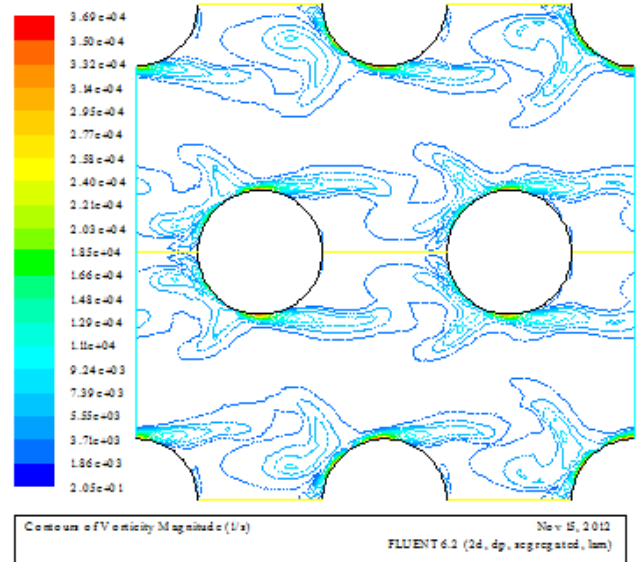


Figure 12 (c)

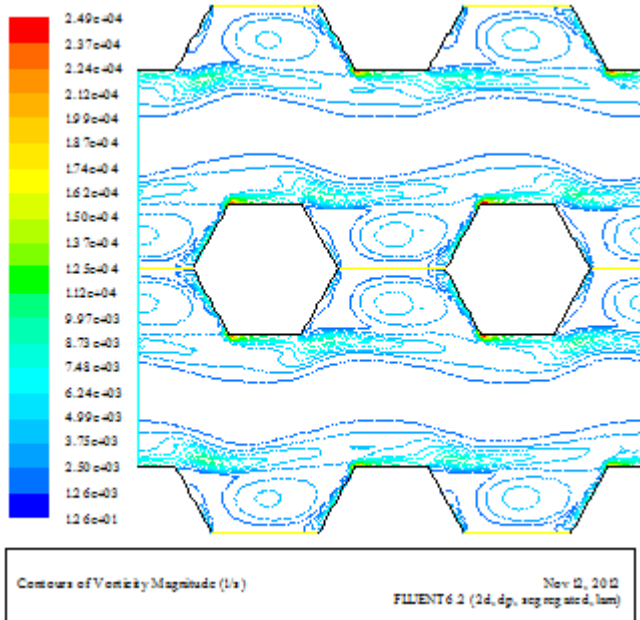


Figure 12 (a)

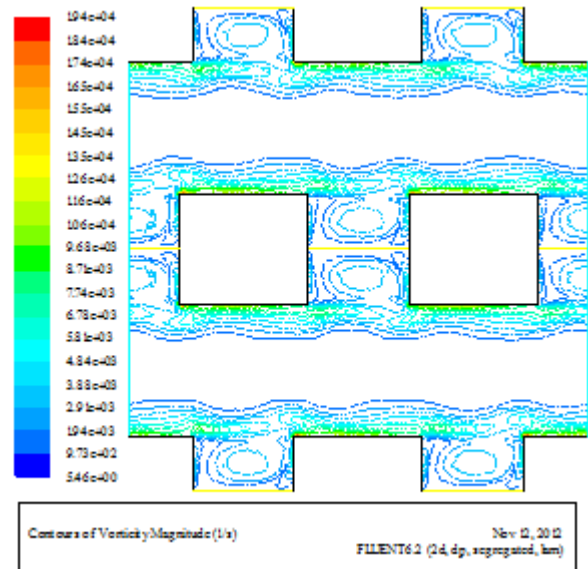


Figure 12 (d)

Figure 12: Vorticity Magnitude at Re=565

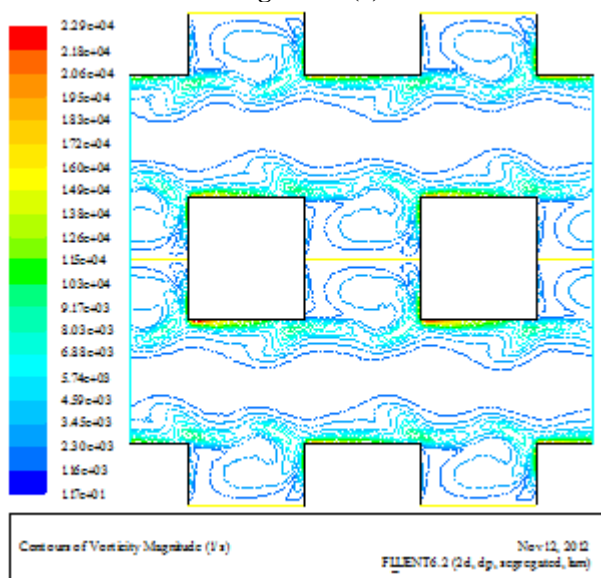


Figure 12 (b)

References

- [1] E. M. Sparrow and E. D. Larson, "Heat Transfer from Pin-Fins Situated in an Oncoming Longitudinal Flow which Turns to Crossflow," International Journal of Heat Mass Transfer, Vol. 25, No. 5, pp. 603-614, 1982.
- [2] E. D. Larson and E. M. Sparrow, "Shorter Communications in Heat Transfer from Pin-Fins Situated in an Oncoming Longitudinal Flow which Turns to Crossflow," International Journal of Heat and Mass Transfer, Vol. 25, No. 5, pp. 723-725, 1982.
- [3] R.W. Keyes, "Heat Transfer in Forced Convection Through Fins," IEEE Transactions on Electron Devices, Vol. 31, No. 9, pp. 1218-1221, September 1984.
- [4] A. Bejan and A. M. Morega, "Optimal Arrays of Pin Fins and Plate Fins in Laminar Forced Convection," Transactions of the ASME, Journal of Heat Transfer, Vol. 115, pp. 75-81, February 1993.
- [5] C. L. Chapman, S. Lee, and B. L. Schmidt, "Thermal Performance of an Elliptical Pin Fin Heatsink,"

- Proceedings of the Tenth IEEE Semiconductor Thermal Measurement and Management Symposium (Semi-Therm), San José, California, February 1-3, pp. 24-31, 1994.
- [6] R. A. Wirtz, W. Chen, and R. Zhou, "Effect of Flow Bypass on the Performance of Longitudinal Fin Heatsinks," Transactions of the ASME, Journal of Electronic Packaging, Vol. 116, pp. 206-211, September 1994.
- [7] H. Iwasaki, T. Sasaki, and M. Ishizuka, "Cooling Performance of Plate Fins for Multichip Modules," IEEE Transaction on Components, Packaging, and Manufacturing Technology - Part A, Vol. 18, No. 3, pp. 592-595, September 1995.
- [8] J. R. Culham, M. M. Yovanovich, and S. Lee, "Thermal Modeling of Isothermal Cuboids and Rectangular Heatsinks Cooled by Natural Convection," IEEE Transactions on Components, Packaging, and Manufacturing Technology -Part A, Vol. 18, No. 3, pp. 559-566, September 1995.
- [9] R. A. Wirtz and D. M. Colban, "Comparison of the Cooling Performance of Staggered and In-Line Arrays of Electronic Packages," Transactions of the ASME, Journal of Electronic Packaging, Vol. 118, No. 1, pp. 27-30, March 1996.
- [10] P. Sathyamurthy, P.W. Runstadler, and S. Lee, "Numerical and Experimental Evaluation of Planar and Staggered Heat Sinks," Proceedings of the Fifth InterSociety Conference on Thermal Phenomena in Electronic Packaging (Itherm), Orlando, Florida, May 28 – June 1, pp. 132-139, 1996.
- [11] R. A. Wirtz, R. Sohal, and H. Wang, "Thermal Performance of Pin-Fin Fan-Sink Assemblies," Transactions of the ASME, Journal of Electronic Packaging, Vol. 119, No. 1, pp. 26-31, March 1997.
- [12] L. W. Zhang et al., "Heat Transfer Enhancement Mechanisms in Inline and Staggered Parallel-Plate Fin Heat Exchanger," International Journal of Heat and Mass Transfer, Vol. 40, No. 10, pp. 2307-2325, 1997.
- [13] A. V. Barrett and I. F. Obinelo, "Characterization of Longitudinal Fin Heatsink Thermal Performance and Flow Bypass Effects Through CFD Methods," Proceedings of the Thirteenth IEEE Semiconductor Thermal Measurement and Management Symposium (Semi-Therm), Austin, Texas, January 28-30, pp. 158-164, 1997.
- [14] D. Soodphakdee, M. Behnia, D. W. Copeland, "A Comparison of Fin Geometries for Heatsinks in Laminar Forced Convection" The International Journal of Microcircuits and Electronic Packaging, , First Quarter, Volume 24, Number 1, pp.68-76 , 2001.
- [15] S. Kakaç ,L.L.Vasiliev,Y. Bayazitoglu,Y. Yener "Microscale Heat Transfer Fundamentals and Applications ",Springer, The Netherlands, 2004, pp. 102.
- [16] Nabati H., Mahmoudi J., "Optimal Pin Fin Heat Exchanger Surface for Pulp and Paper Industry", the Fifth International IMACS Symposium on Mathematical Modeling(5th MATHMOD), February 8 – 10, Vienna University of Technology, Vienna, Austria, 2006.pp.8
- [17] FLUENT/UNS User's Guide, Fluent Incorporated, Lebanon, New Hampshire, 2006.
- [18] O. P. Bergelin, G. A. Brown, and S. C. Doberstein, "Heat Transfer and Fluid Friction during Flow across Banks of Tubes –IV", Transactions of the ASME, Vol. 74, pp. 953-960, August 1952
- [19] T. Nishimura, H. Itoh, K. Ohya, and H. Miyashita, "Experimental Validation of Numerical Analysis of Flow across Tube Banks for Laminar Flow", Journal of Chemical Engineering of Japan, Vol. 24, No. 5, pp. 666-669, 1991.